

Technical Memorandum 2

DATE: June 22, 2004

TO: Ron Mitchum (BCDCOG)
Environmental Technical Advisory Committee

FROM: Bill Martello (JJG)
Steve Davie (TT)

SUBJECT: Charleston Harbor System
Open Boundary Conditions

Introduction

This technical memorandum provides a description of the implementation of open boundary conditions to be used in the development of an EFDC hydrodynamic and water quality model for the Charleston Harbor system, including the Ashley, Cooper and Wando Rivers. Dynamic open boundary conditions are required to provide sea level forcing for the hydrodynamic model while inflowing concentrations boundary conditions are required for the hydrodynamic model's simulation of salinity and temperature and the water quality model's simulation of water quality state variables. No rule exists for the selection of the coastal ocean open boundary location for estuary models. However, the general consensus of experienced modelers, as evidenced by successful published model applications, is that the open boundary should be sufficiently removed from the primary region of interest in the estuary such that the open boundary forcing functions do not over constrain the fundamental physical and biogeochemical processes in the region of interest.

For Charleston Harbor, the region of interest is readily defined to be landward of the mouth of the Harbor, Figure 1. The open boundary should be selected to define a large external region, which provides a buffer between the open boundary conditions and the region of interest. The blue line in Figure 1, illustrates a possible open boundary for the Charleston Harbor, with the buffer region being the area seaward to the coastline and mouth of the harbor. In general the volume of the buffer region should be similar to the volume of the estuary region and its aerial extent should be sufficiently large to allow the dynamics of the estuarine outflow plume in the coastal water to be correctly simulated. This will insure that the correct portion of the water exiting the estuary on ebbing tide will reenter on the next flood tide. If the open boundary were selected at the mouth of the estuary, the boundary conditions would have to empirically incorporate complex dynamics of the estuary-ocean exchange. In many model applications that follow this experiential rule for selection of the open boundary, actual observational data on the open boundary may be sparse or non-existent. This is compensated for by the fact that salinity, temperature and the concentrations of water quality variables are less variable along an open boundary distant from the estuary mouth than they are in the interior of the estuary, where the bulk of observational data normally exist. Also there is a large base of empirical and robust

mathematical approaches to aide in the establishment of open boundary conditions using observational data interior to the open boundary during the process of model calibration. The following sections provide more details on this approach.

Hydrodynamic Open Boundary Conditions

Two types of hydrodynamic open boundary conditions are commonly used in estuarine and coastal ocean modeling. The first is a simplistic specification of the time varying water surface elevation, ζ , along the open boundary

$$\zeta = \zeta_B(s, t) \quad (1)$$

where ζ_B , is the boundary condition, t denotes time and s denotes the tangential coordinate in a normal-tangential coordinates system (n, s) along the boundary and represents the possible accounting for of spatial variations at a given time along the boundary. When observational data to specify the right side of (1) are not available on the open boundary, as is most often the case, it is determined during the calibration of the model. A typical approach is to approximate ζ_B by

$$\zeta_B(t) = A\zeta_O(t + \tau) \quad (2)$$

where ζ_O is an observed water surface elevation record in the estuary region, preferably near the mouth of the estuary, A is an amplitude adjustment factor, and τ is a time phase shift. The values of A and τ are determined by trial and error or linear regression such that when (1) and (2) define the open boundary condition the model correctly predicts the observed water surface elevation, ζ_O . Although generally effective in reproducing observations at the calibration location, (2) fails to provide a boundary condition outside the temporal record of the observation location. The boundary condition (1) is typically used by inexperienced modelers who either lack a sound theoretical background in long wave dynamics or are constrained by the use of models not having a more appropriate option.

A more dynamically correct hydrodynamic open boundary condition is

$$\zeta - \frac{\mathbf{n} \cdot \bar{\mathbf{u}}H}{\sqrt{gH}} = 2\zeta_I(s, t) \quad (3)$$

where \mathbf{n} is the outward normal unit vector along the open boundary, $\bar{\mathbf{u}}$ is the depth average horizontal velocity vector, H is the water depth, g is the acceleration of gravity, and ζ_I is the equivalent amplitude of the incoming wave. The left side of (3) is the characteristic of the incoming wave at the open boundary and follows mathematically from the characteristic form of the shallow water equations. The specification of the incoming wave characteristic allows reflected out going waves generated in the interior of the model domain to pass out of the open boundary without spurious reflection. The use of (1) is well known to create spurious reflection of outgoing waves and attempts are often made to use enhanced friction near the open boundary,

often referred to as a sponge layer, to control the reflection back into the interior. For purely progress incoming waves into a semi-infinite domain it can be readily shown that

$$-\frac{\mathbf{n} \cdot \bar{\mathbf{u}}H}{\sqrt{gH}} = \zeta \quad (4)$$

with (3) reducing to (1) further indicating the inappropriateness of (1) when reflected waves, generated in the interior of the model domain, propagate back out across the open boundary. At first inspection, application of (3) would seem prohibitive since in addition to the water surface elevation, the normal velocity component is required to define the boundary condition on the right side. This problem and the need for observational data at the open boundary can be eliminated and a true predictive boundary condition established if an appropriate calibration procedure, using interior water surface elevation and current meter data, is used to implement the boundary condition (3).

The first step in determining the right side of (3) is its separation and the separation of observational water surface elevation and current meter data into tidal and lower frequency sub-tidal components. Equation (3) becomes

$$\zeta' - \left(\frac{\mathbf{n} \cdot \bar{\mathbf{u}}H}{\sqrt{gH}} \right)' = 2\zeta'_i(s,t) \quad (5a)$$

$$\zeta'' - \left(\frac{\mathbf{n} \cdot \bar{\mathbf{u}}H}{\sqrt{gH}} \right)'' = 2\zeta''_i(s,t) \quad (5b)$$

and the observational data become

$$\begin{aligned} \zeta_o &= \zeta'_o + \zeta''_o \\ \bar{\mathbf{u}}_o &= \bar{\mathbf{u}}'_o + \bar{\mathbf{u}}''_o \\ \bar{\mathbf{v}}_o &= \bar{\mathbf{v}}'_o + \bar{\mathbf{v}}''_o \end{aligned} \quad (6)$$

where the single and double primes denote the tidal and sub-tidal frequency components, respectively. For the observational data, the separation is readily accomplished using appropriate high and low pass filtering. Low frequency water surface elevation variation in estuaries is driven primarily by local atmospheric variability and low frequency sea level variability with sea level variability being dominant except in very large estuaries such as the Chesapeake Bay. Low frequency sea level variability on the Atlantic Coast of the US occurs normally at scales of 2.5 to 10 days and is primarily associated with the passage of frontal systems. A strong correlation exist between along shore wind speed and direction and low frequency sea level, typically allowing low frequency sea level to be predicted for non-observed periods using wind observations. The other characteristic feature of low frequency sea level variability is that the low frequencies result in very long wave lengths, allowing the low frequency sea level on the open boundary to be well approximated by low frequency sea level observations near the mouth

of the estuary. The propagation of low frequency sea level generated waves into estuaries tends to be primarily progressive with (4) being appropriate. These two feature allow the low frequency open boundary condition (5b) to be well approximated as

$$\zeta'' - \left(\frac{\mathbf{n} \cdot \bar{\mathbf{u}} H}{\sqrt{gH}} \right)'' = 2\zeta_o''(t) \quad (7)$$

along the entire open boundary using an interior observation of low frequency sea level in the modeling domain. For the Charleston Harbor hydrodynamic model the low frequency open boundary condition will use the low pass filtered NOAA tide gauge record at the entrance of the Cooper River. Figure 2 shows a 35-day period of the instantaneous NOAA tide gauge record and its sub-tidal component at the entrance of the Cooper River, with the corresponding tidal component shown in Figure 3. Figure 4 shows a year long record of the sub-tidal component of sea level, extracted from the NOAA tide gauge record at the entrance to the Cooper River.

The tidal component of the open boundary condition is best expressed in harmonic form

$$\zeta'_I(s, t) = \sum_{m=1}^M \left(\begin{aligned} & \left(A_{c0} + A_{c1}s + A_{c2}s^2 + \dots \right)_m \cos(\omega_m t) \\ & + \left(A_{s0} + A_{s1}s + A_{s2}s^2 + \dots \right)_m \sin(\omega_m t) \end{aligned} \right) \quad (8)$$

where M is the number of harmonics, A_c and A_s are the cosine and sine amplitudes for each harmonic component, s is the tangential distance coordinate along the open boundary, and ω_m is the harmonic component frequency. Equation (8) shows a quadratic variation of the cosine and sine amplitudes along the open boundary, which can be extended to higher order for long open boundaries or truncated to linear or constant behavior for short open boundaries. The calibration of the tidal open boundary condition involves selection the cosine and sine amplitudes for each tidal constituent. For example if the quadratic dependence shown above is used, there are 6 amplitudes to be determined for each constituent. Typically 5 or 6 constituents are required to represent mixed tides along the US Atlantic coast. The tidal component of each observational record of surface elevation and velocity can also be expressed in harmonic form

$$\begin{aligned} \zeta'_O(t) &= \sum_{m=1}^M (Z_{cm} \cos(\omega_m t) + Z_{sm} \sin(\omega_m t)) \\ \vec{u}'_O(t) &= \sum_{m=1}^M (U_{cm} \cos(\omega_m t) + U_{sm} \sin(\omega_m t)) \\ \vec{v}'_O(t) &= \sum_{m=1}^M (V_{cm} \cos(\omega_m t) + V_{sm} \sin(\omega_m t)) \end{aligned} \quad (9)$$

with the harmonic amplitudes, Z_c , Z_s , U_c , U_s , V_c , and V_s readily determined by least squares harmonic analysis of the observational time series. Table 1 shows the water surface elevation tidal harmonic components for the NOAA tide gauge at the entrance of the Cooper River near the Customs House.

The open boundary condition harmonic amplitudes in (8) can be determined during calibration using a least squares minimization procedure. This procedure minimizes an objective function of the form

$$R = \frac{1}{2} \sum_{m=1}^M W_m \left((P_{cm} - O_{cm})^2 + (P_{sm} - O_{sm})^2 \right) \quad (10)$$

where P and O represent model predictions and observations, respectively of Z , U , and V at M locations in the interior of the model domain. The objective function can be expanded in a second order Taylor series in the unknown A coefficients in (8) to give

$$R(\mathbf{A}) = R(\mathbf{A}^*) + (\nabla R)^T (\mathbf{A} - \mathbf{A}^*) + \frac{1}{2} (\mathbf{A} - \mathbf{A}^*)^T \mathbf{H} (\mathbf{A} - \mathbf{A}^*) \quad (11)$$

The initial guess of the coefficients, denote by $*$, defines the origin of the expansion. Other terms in (11) are defined by

$$\begin{aligned} \mathbf{A} &= \{A_i\} \\ \nabla R &= \left\{ \left. \frac{\partial R}{\partial A_i} \right|_{\mathbf{A}^*} \right\} \\ \mathbf{H} &= \left[\left. \frac{\partial^2 R}{\partial A_i \partial A_j} \right|_{\mathbf{A}^*} \right] \end{aligned} \quad (12)$$

with \mathbf{A} being an ordered column vector containing the A coefficients, ∇R a corresponding ordered column vector of the gradients of the objective function with respect to the A coefficients, and \mathbf{H} the Hessian matrix of cross gradients. Minimizing (11) with respect to the A coefficients gives

$$\mathbf{H}(\mathbf{A}^{opt} - \mathbf{A}^*) = -(\nabla R)^T \quad (13)$$

Using (12) allows (13) to be written in the form

$$\left[\left. \frac{\partial^2 R}{\partial A_i \partial A_j} \right|_{\mathbf{A}^*} \right] \{A_j^{opt}\} = - \left\{ \left. \frac{\partial R}{\partial A_i} \right|_{\mathbf{A}^*} \right\} \quad (14)$$

corresponding to a set of linear equations which can be solved for the optimum set of A coefficients provided the Hessian matrix and the gradient vector can be estimated.

The Hessian matrix and the gradient vector can be readily estimated by parameter perturbation about the initial coefficient set, A^* . The gradients can be determined using one sided

$$\left. \frac{\partial R}{\partial A_i} \right|_{\square} \frac{\partial R}{\partial A_i} \Bigg|_* = \frac{R(A_i^* + \delta A_i, A_{j,j \neq i}^*) - R(A_i^*)}{\delta A_i} \quad (15)$$

or centered

$$\left. \frac{\partial R}{\partial A_i} \right|_{\square} \frac{\partial R}{\partial A_i} \Bigg|_* = \frac{R(A_i^* + \delta A_i, A_{j,j \neq i}^*) - R(A_i^* - \delta A_i, A_{j,j \neq i}^*)}{2\delta A_i} \quad (16)$$

difference approximations. The diagonal components of the Hessian are determined by

$$\left. \frac{\partial^2 R}{\partial A_i \partial A_i} \right|_* = \frac{R(A_i^* + \delta A_i, A_{j,j \neq i}^*) - 2R(A_i^*) + R(A_i^* - \delta A_i, A_{j,j \neq i}^*)}{(\delta A_i)^2} \quad (17)$$

which corresponds to a center second derivative. The off-diagonal components of the Hessian can be determined by one sided

$$\left. \frac{\partial^2 R}{\partial A_i \partial A_j} \right|_{i \neq j} \Bigg|_* = \frac{1}{\delta A_i \delta A_j} \left(\begin{array}{l} R(A_i^* + \delta A_i, A_j^* + \delta A_j, A_{k,k \neq i \neq j}^*) + R(A_i^*) \\ -R(A_j^* + \delta A_j, A_i^*, A_{k,k \neq j}^*) - R(A_i^* + \delta A_i, A_{k,k \neq i}^*) \end{array} \right) \quad (18)$$

or centered

$$\left. \frac{\partial^2 R}{\partial A_i \partial A_j} \right|_{i \neq j} \Bigg|_* = \frac{1}{4\delta A_i \delta A_j} \left(\begin{array}{l} R(A_i^* + \delta A_i, A_j^* + \delta A_j, A_{k,k \neq i \neq j}^*) \\ +R(A_i^* - \delta A_i, A_j^* - \delta A_j, A_{k,k \neq i \neq j}^*) \\ -R(A_i^* - \delta A_i, A_j^* + \delta A_j, A_{k,k \neq i \neq j}^*) \\ -R(A_i^* + \delta A_i, A_j^* - \delta A_j, A_{k,k \neq i \neq j}^*) \end{array} \right) \quad (19)$$

differences approximations. Figure 5 shows the number of model runs required to determine a given number of model parameters using the directed minimization approach defined by equations (14) through (19). Since tides in Charleston Harbor are dominated by the *M2* semi-diurnal constituent, as shown in Table 1, the estimation of the *A* coefficients can be done constituent by constituent beginning with the *M2* constituent. For quadratic variation of the cosine and sine amplitudes along the open boundary, six *A* coefficients are required for each constituent. The number of model runs required for each constituent determination is 28. If a linear variation is used along the open boundary, only four *A* coefficients are required per constituent and the number of models runs for each constituent is reduced to 15. The length of each model run be approximately 42 days corresponding to a 14 day spin-up period followed by a 28 day spring-neap cycle necessary to separate diurnal and semi-diurnal tidal constituents using least squares harmonic analysis.

Table 1. Harmonic Components of Tidal Water Surface Elevation for NOAA Gauge at entrance of Cooper River near Customs House.

Tidal Constituent	Period (seconds)	Cos Amp (meters)	Sin Amp (meters)	Abs Amp (meters)	Phase (seconds)
M2	44,714	-0.239	0.756	0.793	13,356
N2	43,200	-0.046	-0.110	0.119	29,656
S2	45,570	-0.138	-0.103	0.172	27,428
K2	43,082	0.018	0.016	0.024	5,009
K1	86,164	-0.035	0.084	0.091	26,994
O1	92,950	0.057	0.031	0.065	7,342
P1	86,637	-0.26	0.023	0.034	33,294

Salinity, Temperature and Water Quality Open Boundary Conditions

When water flows inward across the open boundary, into the model domain, its salinity, temperature and the concentration of water quality state variables must be specified. The corresponding boundary condition is

$$C = C_B(s, t) \quad ; \quad \mathbf{n} \bullet \mathbf{u} < 0 \quad (20)$$

where C represents salinity, temperature or water quality state variable concentration, B denotes the boundary value, \mathbf{n} is the outward normal vector and \mathbf{u} is the horizontal velocity vector along the open boundary. For tidal and other reversing flow open boundaries, the boundary concentration can be specified as

$$C_B(s, t) = C_{LO} + (C_{BU} - C_{LO}) \left(\frac{t - T_{OI}}{T_R} \right) \quad ; \quad T_{OI} < t \leq T_{OI} + T_R \quad (21)$$

$$C_B(s, t) = C_{BU} \quad ; \quad T_{OI} + T_R < t < T_{IO}$$

where

$$C_{LO} = C_{LO}(s, T_{OI}) = \text{last outflowing concentration}$$

$$C_{BU} = C_{BU}(s, t) = \text{ultimate inflowing concentration}$$

$$T_{OI} = T_{OI}(s) = \text{time of change from outflow to inflow} \quad (22)$$

$$T_{IO} = T_{IO}(s) = \text{time of change from inflow to outflow}$$

$$T_R(s) = \text{recovery time}$$

The period of inflow along the open boundary is determined by.

$$\mathbf{n} \cdot \mathbf{u} \leq 0 \quad ; \quad T_{OI} < t < T_{IO} \quad (23)$$

The boundary concentration (21) essentially represents a quasi-linear transition from the last out flowing concentration to the ultimate in flowing concentration over a recovery interval, T_R , followed by inflow of the ultimate inflow concentration, C_{BU} , over the remainder of the inflow period. Specification of the open boundary concentration boundary condition then requires defining the recovery interval and the ultimate inflowing concentration. If the open boundary buffer region is sufficiently large, the recovery interval exerts little influence on concentrations in the interior region of interest and is typically set within the range of one to three hours to avoid an abrupt change in concentration. A large open boundary region also allows the ultimate inflow concentration to be set to represent sub-tidal to longer seasonal time scale variability.

If sufficient observational data is not available in the immediate vicinity of the open boundary, the minimization procedure describe in the preceding section can be employed to develop time series for the ultimate inflowing open boundary concentration during the model calibration process. The cost function in this case takes the form

$$R = \frac{1}{2} \sum_{m=1}^M \sum_{n=1}^N W_{m,n} (P_{m,n} - O_{m,n})^2 \quad (24)$$

where P and O represent model predicted and observed concentrations, respectively, at M observation locations and N observation times. The ultimate inflowing concentration is specified by a prescribed function of position along the open boundary and time. A typical specification might be of the form

$$C_{BU}(s, t) = \psi(s) \chi(t - \tau(s)) \quad (25)$$

which represents a base time function $\chi(t)$, whose amplitude and phase are modified along the open boundary by the spatial functions $\psi(s)$ and $\tau(s)$. The simplest spatial functions are polynomials

$$\begin{aligned} \psi(s) &= \sum_{k=0}^K \psi_k s^k \\ \tau(s) &= \sum_{k=0}^K \tau_k s^k \end{aligned} \quad (26)$$

whose coefficients can be determined using the minimization procedure corresponding to equations (11) through (19) in the preceding section with the Λ parameters defined by

$$\mathbf{A} = \begin{Bmatrix} \psi_k \\ \tau_k \end{Bmatrix} \quad (27)$$

The methodology for developing the base time function, $\chi(t)$, is generally different for salinity, temperature, and water quality state variables and will now be discussed.

The primary choice in developing a base time function for the salinity open boundary condition is the use of observational data from the interior of estuary or from the exterior coastal region. The salinity at interior locations in an estuary responds to the open boundary condition, tidal variability at semi-diurnal, diurnal, and spring-neap time scales, and net fresh water inflow from rivers and other sources including runoff, storm water discharges, and waste water treatment plant discharges. Figure 6 shows a 30 day record of salinity at USGS station near the Customs House at the entrance to the Cooper River, Charleston Harbor. The salinity exhibits a strong tidal signal as evident by comparison with the corresponding water elevation record in Figure 7. The salinity record in Figure 6 shows a marked drop in salinity between days 57 and 62, which cannot be attributed to tidal variability. Figure 8 shows the corresponding record of daily rainfall at Charleston Air Force Base, while Figures 9 and 10 show the corresponding records of daily flow and preceding 5 day moving average flow, respectively, in the Cooper River below Pinopolis Dam. The high rainfall on days 56 and 57 tend to indicate that early phase of the salinity reduction is most likely associated with localized freshwater run off, in particular a large storm water discharge near the station, while the later phase is influenced by increased freshwater discharge from the Pinopolis dam. With a large open boundary buffer region between the mouth of the harbor and the open boundary, events such as these should exert marginal influence on the open boundary salinity.

Salinity offshore from the mouth of an estuary responds primarily to seasonal scale variations in net freshwater discharge from the estuary of interest and to varying extents from other nearby estuaries along the coastline. This is illustrated in Figure 11, which shows a two-year record of salinity at a station approximately 30 Km southeast of the mouth of the Savannah River as well as the freshwater discharge in the Savannah River. The reduction on offshore salinity is response to high winter and spring flows in the Savannah is clearly evident. Unlike the Savannah and many other riverine estuaries along the US East coast, freshwater discharge through the Charleston Harbor is highly regulated by releases from the Pinopolis Dam on the west branch of the Cooper River. Figure 12 shows daily flows in the Cooper River, below Pinopolis Dam for 2003. The mean flow for 2003 is 145 cms with a standard deviation of 29 cms. Although the flow is highly variable, primarily at weekly time scales, a strong seasonal signal like that exhibited by the Savannah River, is absent. The absence of seasonal variability in the major freshwater inflow to the Charleston Harbor system suggests that the base time function for the salinity open boundary condition will exhibit a rather low degree of variability and can be developed from either interior or exterior salinity observations. If interior observations are used, they should be near the bottom of the water column and include only the peak value observed during a lunar diurnal period. Observational data that is influenced by fresh water inflows close to the observation station should also be excluded. Figure 13 shows lunar diurnal peak salinities over a 30-day period extracted from hourly salinity data shown in Figure 6. Data from the period influenced by the rainfall event was excluded. The average of the peak salinities over this period is approximately 28 psu. An extension of this method using longer salinity observation

records at the USGS Customs House station and Fort Sumter station will be used to develop a base time function for the Charleston Harbor salinity open boundary condition.

The base time function for the temperature open boundary condition can be developed by low pass filtering or Fourier analysis of water temperature observational records from locations within or near the model domain. Figure 14 shows the 30-day record of temperature at the USGS Customs House station at the entrance of the Cooper River. Temperature in estuaries tends to vary slowly in the horizontal direction as evident from the absence of significant tidal time scale variability in Figure 14. Figure 15 shows a four-year record of hourly temperature observations at the NOAA tide gauge near the Customs House at the entrance to the Cooper River, Charleston Harbor. The Fourier approximation to this temperature record, also shown in Figure 15 is suitable for use as base time function for the temperature open boundary condition.

When a full thermal simulation is performed in the hydrodynamic model, inaccuracies in the temperature boundary condition are rapidly eliminated in the buffer region due to the tendency of the water temperature to come into dynamic equilibrium with hourly time scale varying atmospheric heat exchange and solar radiation forcing the thermal simulation.

The development of base time functions for water quality state variables follows that used for temperature. The primary difference is that observational data for the water quality state variables, with the possible exception of dissolved oxygen, is typically sparse and at weekly to monthly intervals rather than hourly intervals. In this case, the extrapolation of the base time function developed from interior observations to the open boundary, using (25) and (26) is more critical than for temperature.

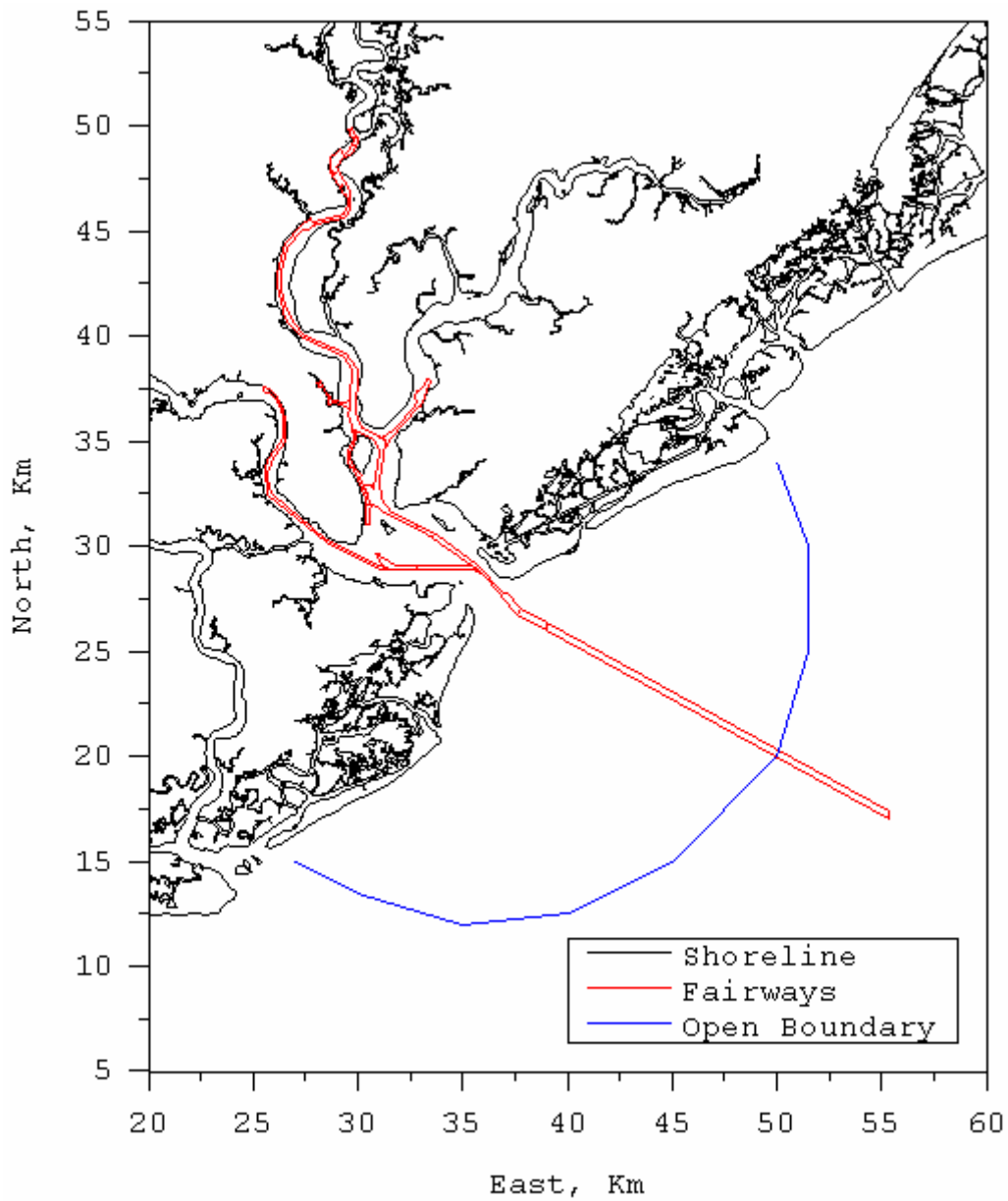


Figure 1. Charleston Harbor region shoreline with navigation fairways and approximate model domain open boundary.

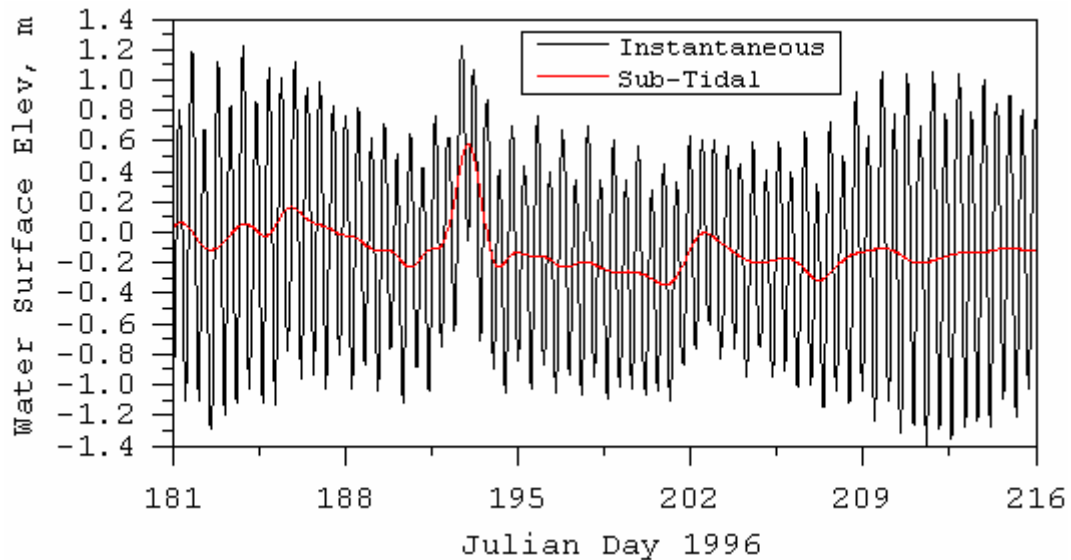


Figure 2. Instantaneous and sub-tidal water surface elevation, relative to local mean sea level, at the NOAA tide gauge near the Customs House at the entrance to the Cooper River, Charleston Harbor.

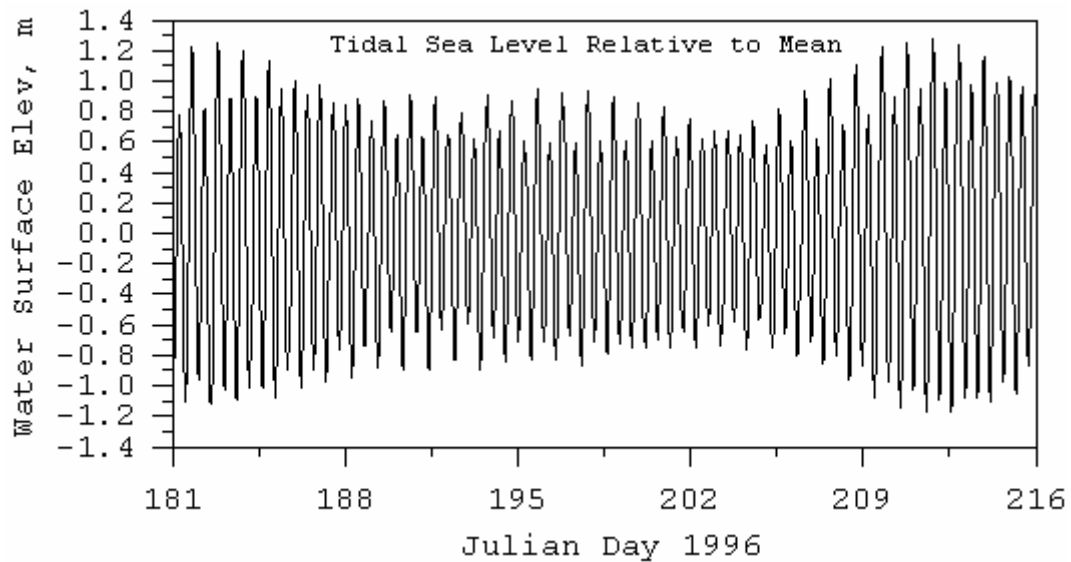


Figure 3. Tidal component of water surface elevation, relative to local mean sea level, at the NOAA tide gauge near the Customs House at the entrance to the Cooper River, Charleston Harbor.

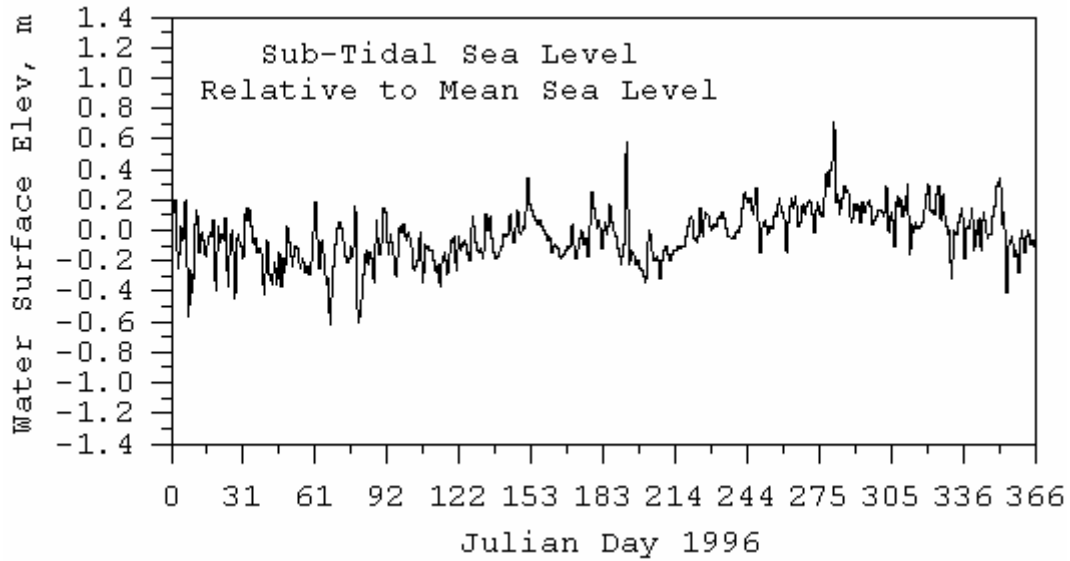


Figure 4. Sub-tidal water surface elevation, relative to local mean sea level, at the NOAA tide gauge near the Customs House at the entrance to the Cooper River, Charleston Harbor.

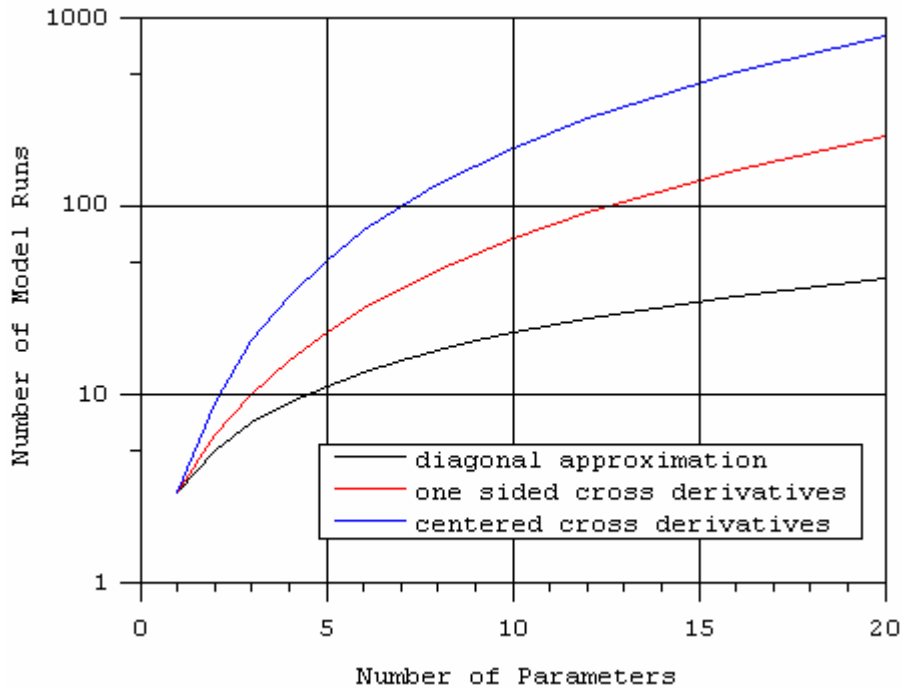


Figure 5. Number of model runs required to determine a specific number of model parameters using direct minimization.

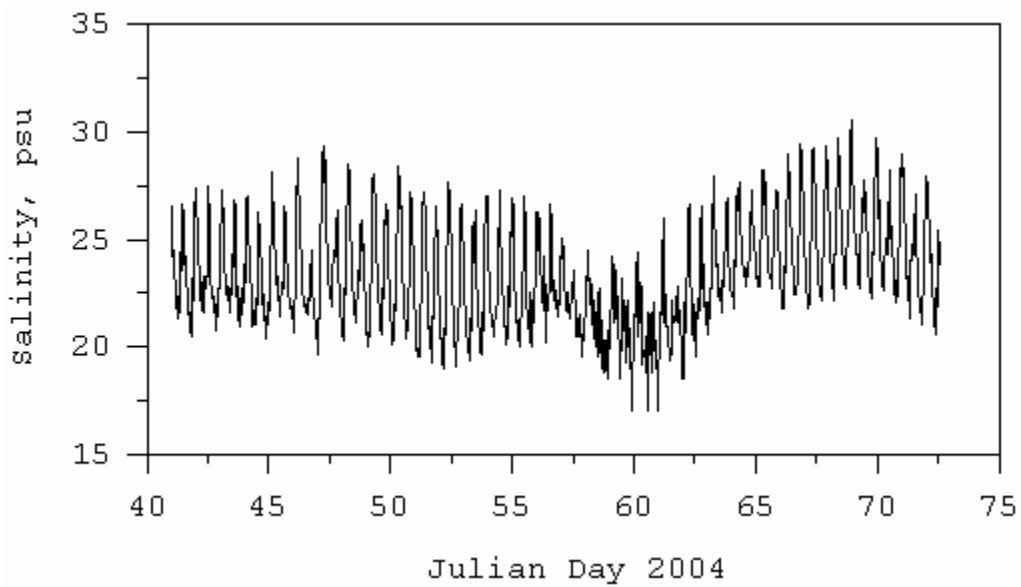


Figure 6. Thirty day record of salinity at USGS station near the Customs House at the entrance to the Cooper River, Charleston Harbor.

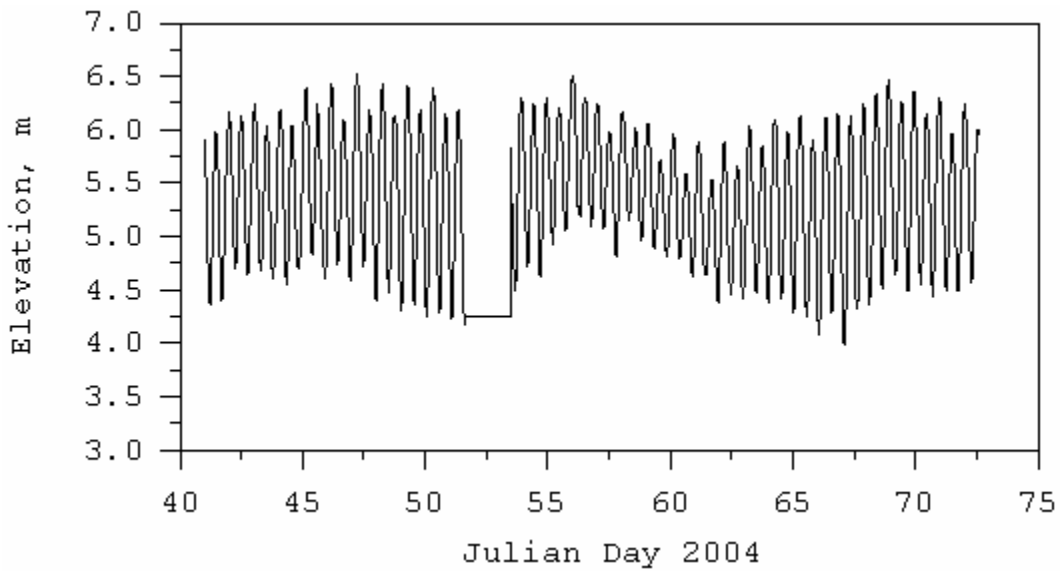


Figure 7. Thirty day record of water surface elevation at USGS station near the Customs House at the entrance to the Cooper River, Charleston Harbor.

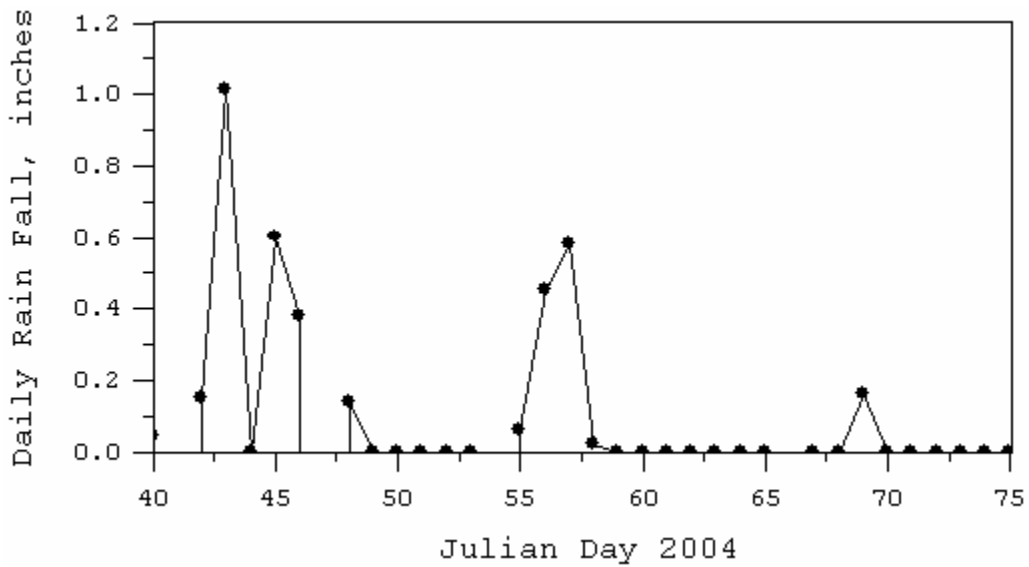


Figure 8. Thirty day record of rainfall at Charleston Air Force Base.

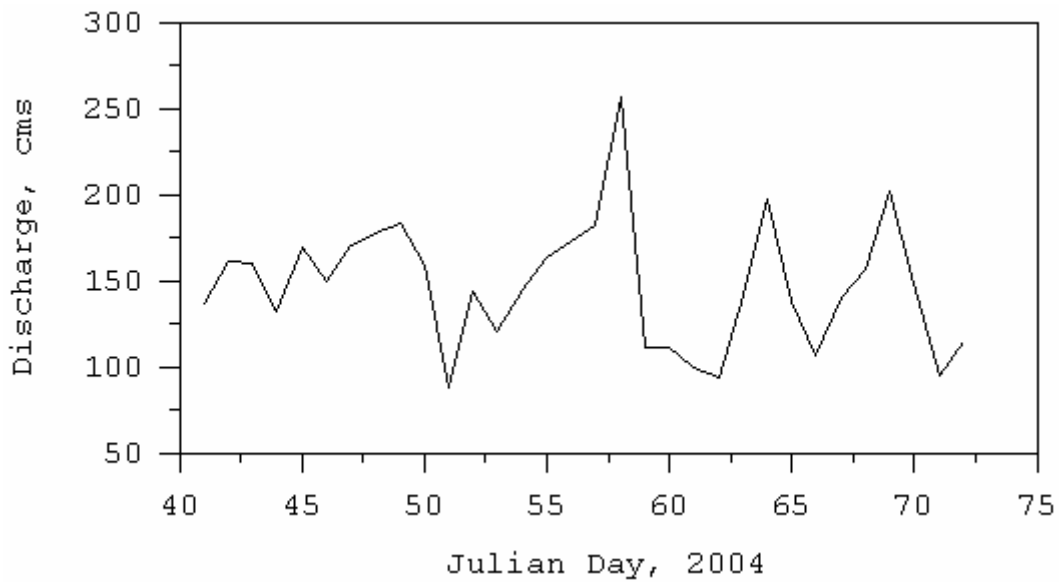


Figure 9. Thirty day record of flow in the Cooper River below Pinopolis Dam.

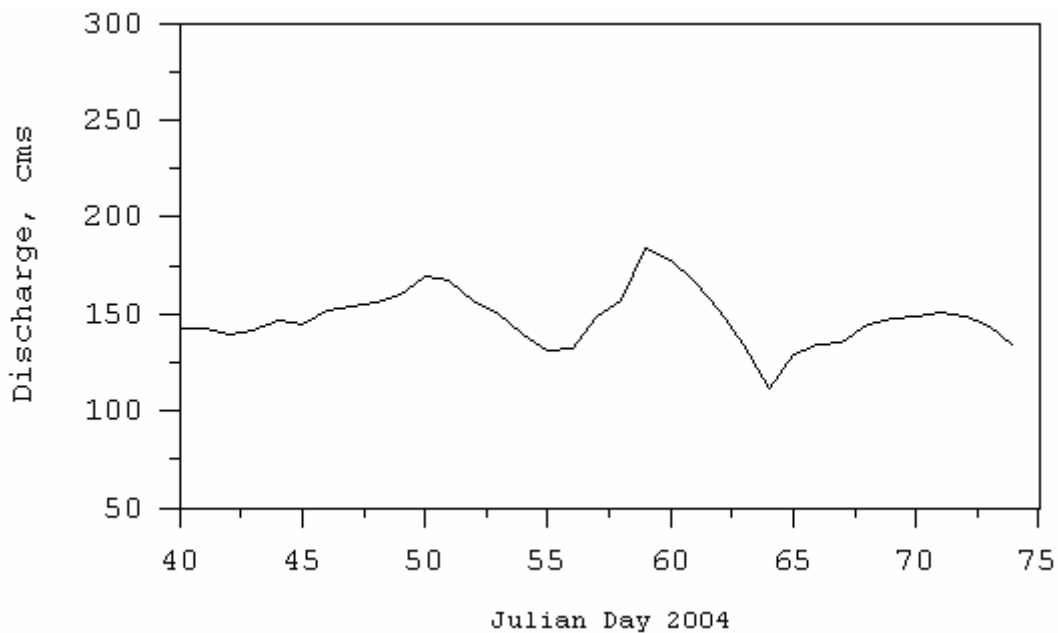


Figure 10. Five day moving average of thirty day record of flow in the Cooper River below Pinopolis Dam.

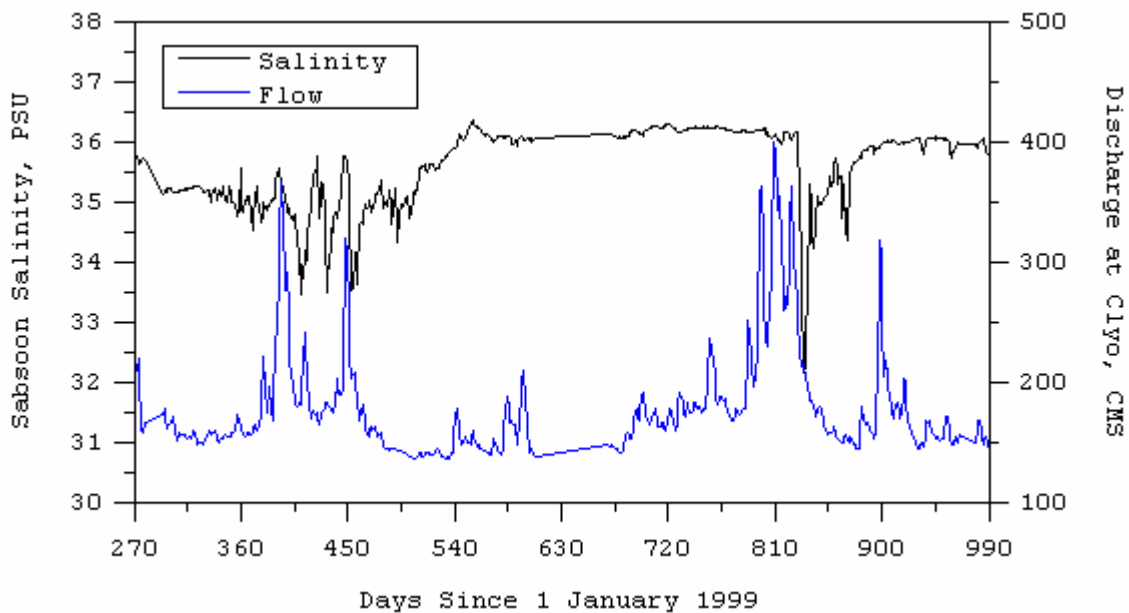


Figure 11. Sabsoon station R2 salinity and Savannah River discharge at Clyo. Note salinity data is missing between approximately days 618 and 670.

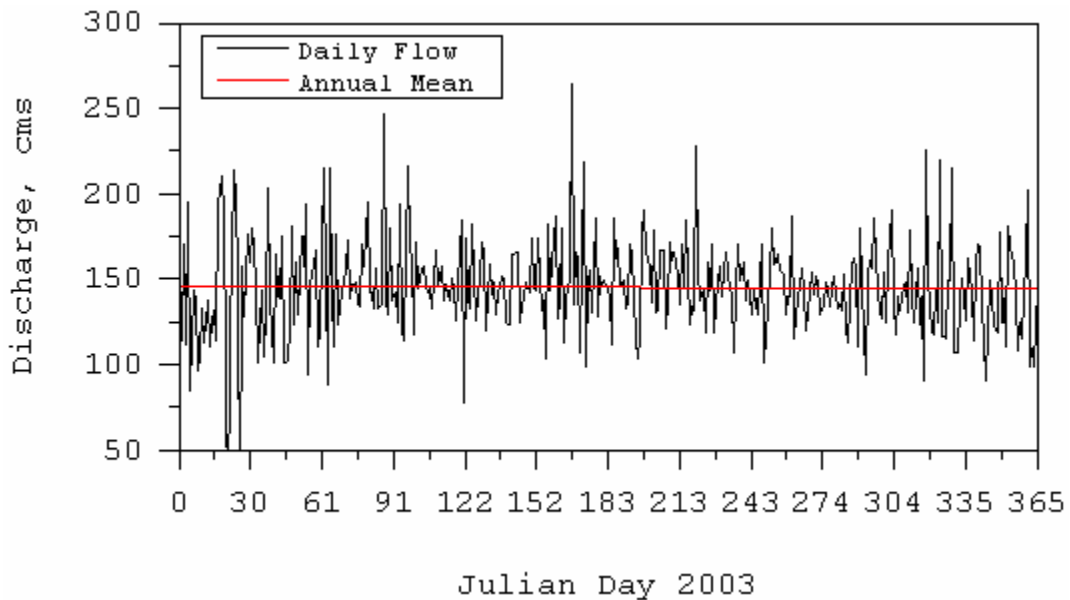


Figure 12. Annual daily flow for 2003 in the Cooper River below Pinopolis Dam.

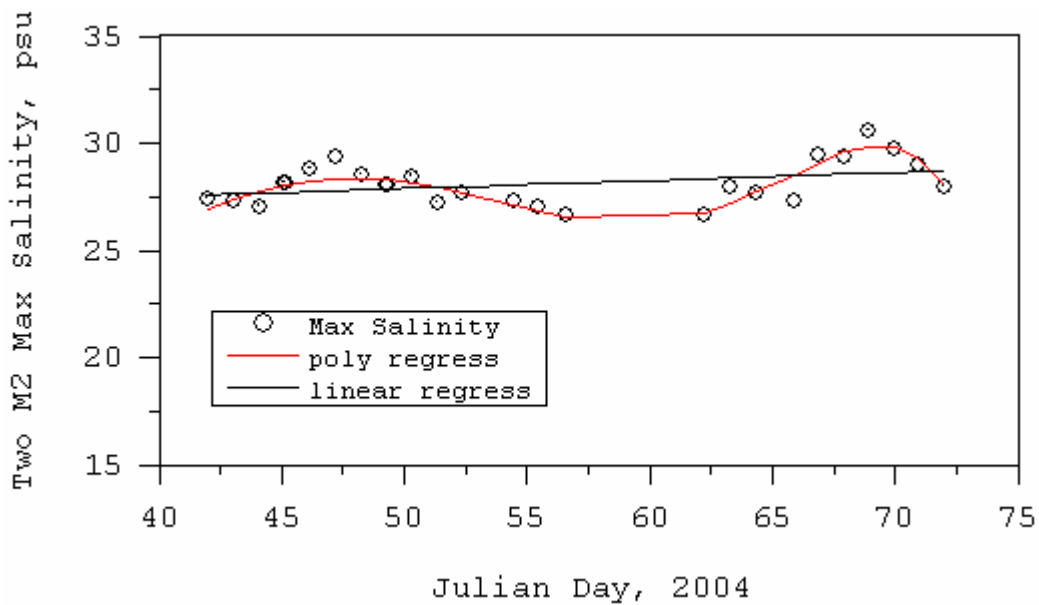


Figure 13. Lunar diurnal peak salinity at USGS station near the Customs House at the entrance to the Cooper River, Charleston Harbor, based on data shown in Figure 6 with data between days 54 and 62 excluded.

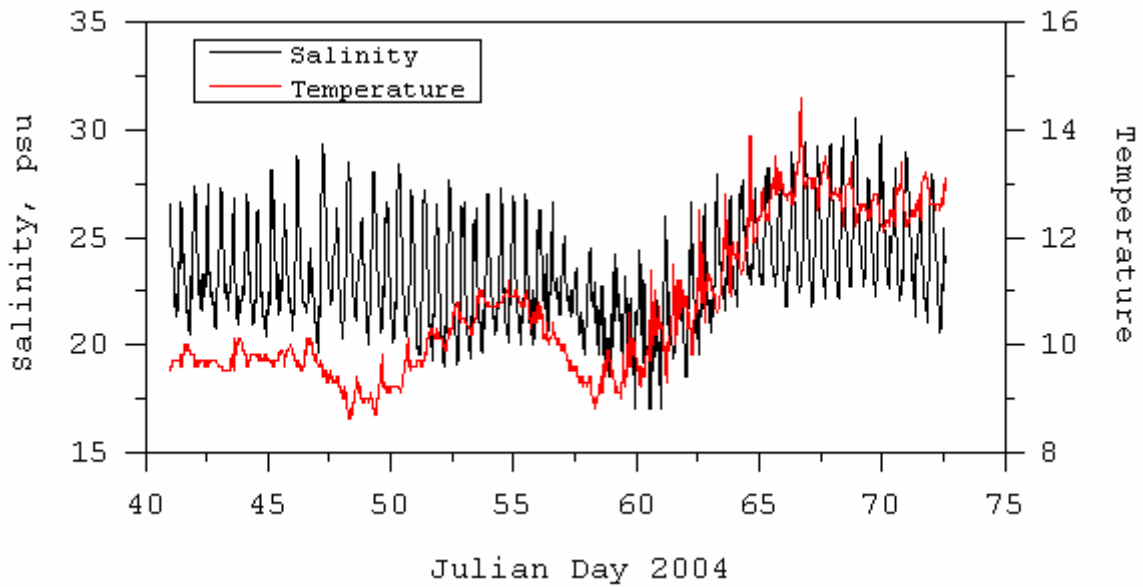


Figure 14. Thirty day record of salinity and temperature at USGS station near the Customs House at the entrance to the Cooper River, Charleston Harbor.

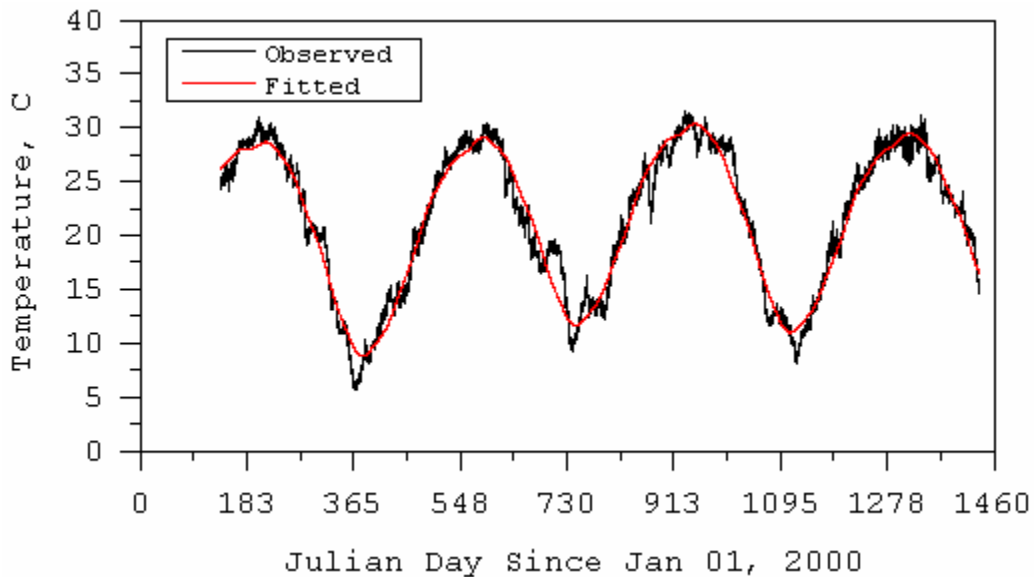


Figure 15. Four year record of temperature at the NOAA tide gauge near the Customs House at the entrance to the Cooper River, Charleston Harbor and its seasonal to annual time scale Fourier fit.